Supplementary Information

Enhanced toluene sensing performances over commercial Co_3O_4 modulated by oxygen vacancy via $NaBH_4$-assisted reduction approach

Liang Zhao, Congcong Xin, Zhimin Yang, Yaqing Zhang, Yunpeng Xing, Zefeng Wei, Teng Fei, Sen Liu*, Tong Zhang*

State Key Laboratory on Integrated Optoelectronics, College of Electronic Science and Engineering, Jilin University, Changchun 130012, P.R. China

*Corresponding authors: E-mail: liusen@jlu.edu.cn (S. Liu); zhangtong@jlu.edu.cn (T. Zhang). Fax: +86 431 85168270; Tel: +86 431 85168385

Table of Contents

Electrochemical characterizations

The measurements were carried out by a typical three-electrode system, including a platinum wire as counter electrode, a Ag/AgCl electrode as reference electrode, and sensing materials modified fluorine doped tin oxide (FTO) as working electrode. The working electrode was prepared as follows: 20 mg of sample and 25 μL of naphthol solution were dispersed in 50 μL of deionized water, and the mixture was sonicated for 5 min. After complete mixing, the slurry was dropped evenly onto a FTO electrode and the coated electrode was dried in air for 12 h.

The Mott−Schottky curve was obtained from the impedance test in the dark at room temperature. A fundamental frequency of 500 Hz and the sweeping potential was from 0.2 to 0.8 V at a scan rate of 50 mV s^{-1}. The electrolyte used here was 0.1 M NaOH aqueous solution, and alternating potential sweep scan was done until the plot tendency of the inverse capacitance remained stable.

The RHE converted from potentials vs Ag/AgCl (0.5 M Na_2SO_4 solution) was obtained using the following relationship:

$$E_{RHE} = E_{Ag/AgCl} + 0.2V.$$

UV/Vis spectra measurements

From the Tauc relationship, the band gap was calculated using following equation:

$$(\alpha h\nu)^{1/n} = A(h\nu - E_g).$$

In the equation, α represents the absorption coefficient, h represents Planck's constant, ν represents the photon frequency, A represents a constant, E_g represents the bandgap, and n represents a power factor that depends on the type of transition, which takes the value of 1/2 and 2 for direct and indirect transition, respectively. E_{CB} was calculated according to following equation:

$$E_{CB} = E_{VB} + E_g$$

Table S1 The parameters for synthesis of Co_3O_4, Co_3O_4-R-1, Co_3O_4-R-3, Co_3O_4-R-5, Co_3O_4-R-7 and Co_3O_4-R-9 samples.

Sample	Co_3O_4 (mg)	$NaBH_4$ (mg)	H_2O (mL)	$NaBH_4$ (mol/L)
Co_3O_4	250	-	12.5	-
Co_3O_4-R-1	250	47.3	12.5	0.1
Co_3O_4-R-3	250	141.9	12.5	0.3
Co_3O_4-R-5	250	236.5	12.5	0.5
Co_3O_4-R-7	250	331.0	12.5	0.7
Co_3O_4-R-9	250	425.6	12.5	0.9

Table S2 The detailed structure parameters of Co_3O_4 and Co_3O_4-R-5.

Sample	BET surface area (m^2/g)	Pore size (nm)	Pore volume (cm^3/g)
Co_3O_4	2.8	6.00	0.04
Co_3O_4-R-5	10.7	6.80	0.05

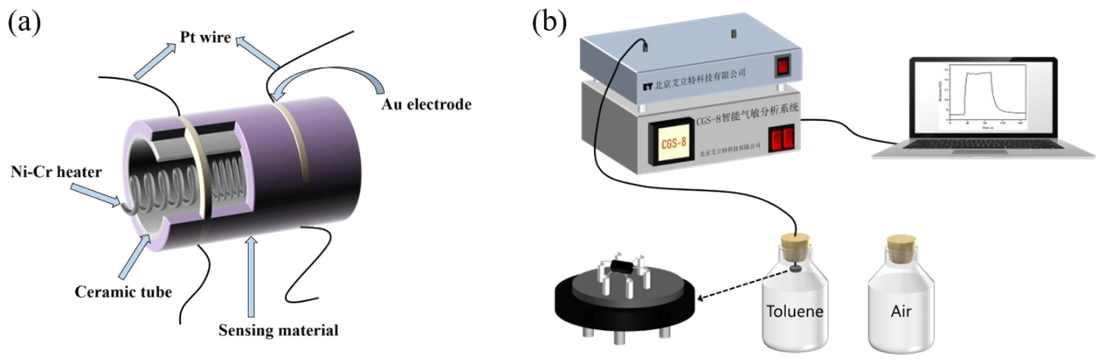

Figure S1 (a) The schematic structure of the gas sensor, and (b) the schematic illustration of gas testing process.

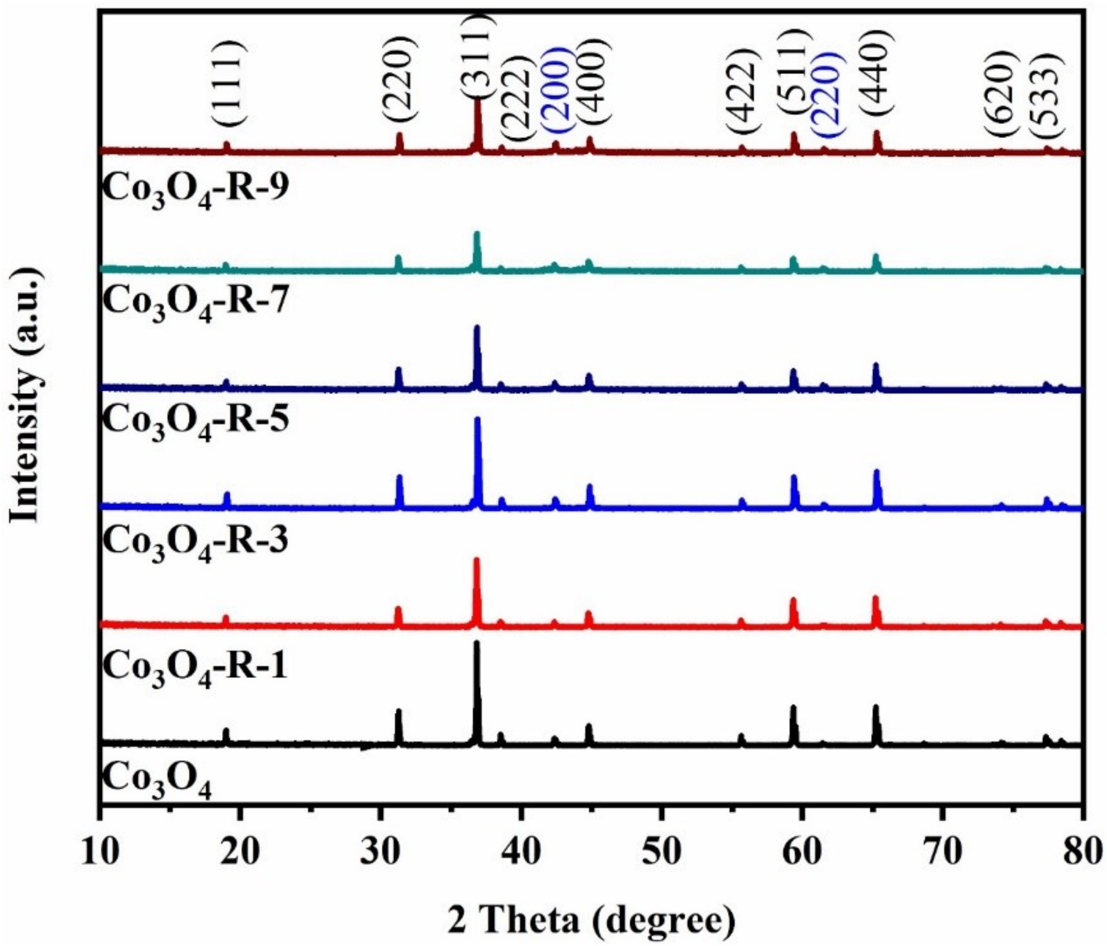

Figure S2 XRD patterns of Co_3O_4, Co_3O_4-R-1, Co_3O_4-R-3, Co_3O_4-R-5, Co_3O_4-R-7, Co_3O_4-R-9.

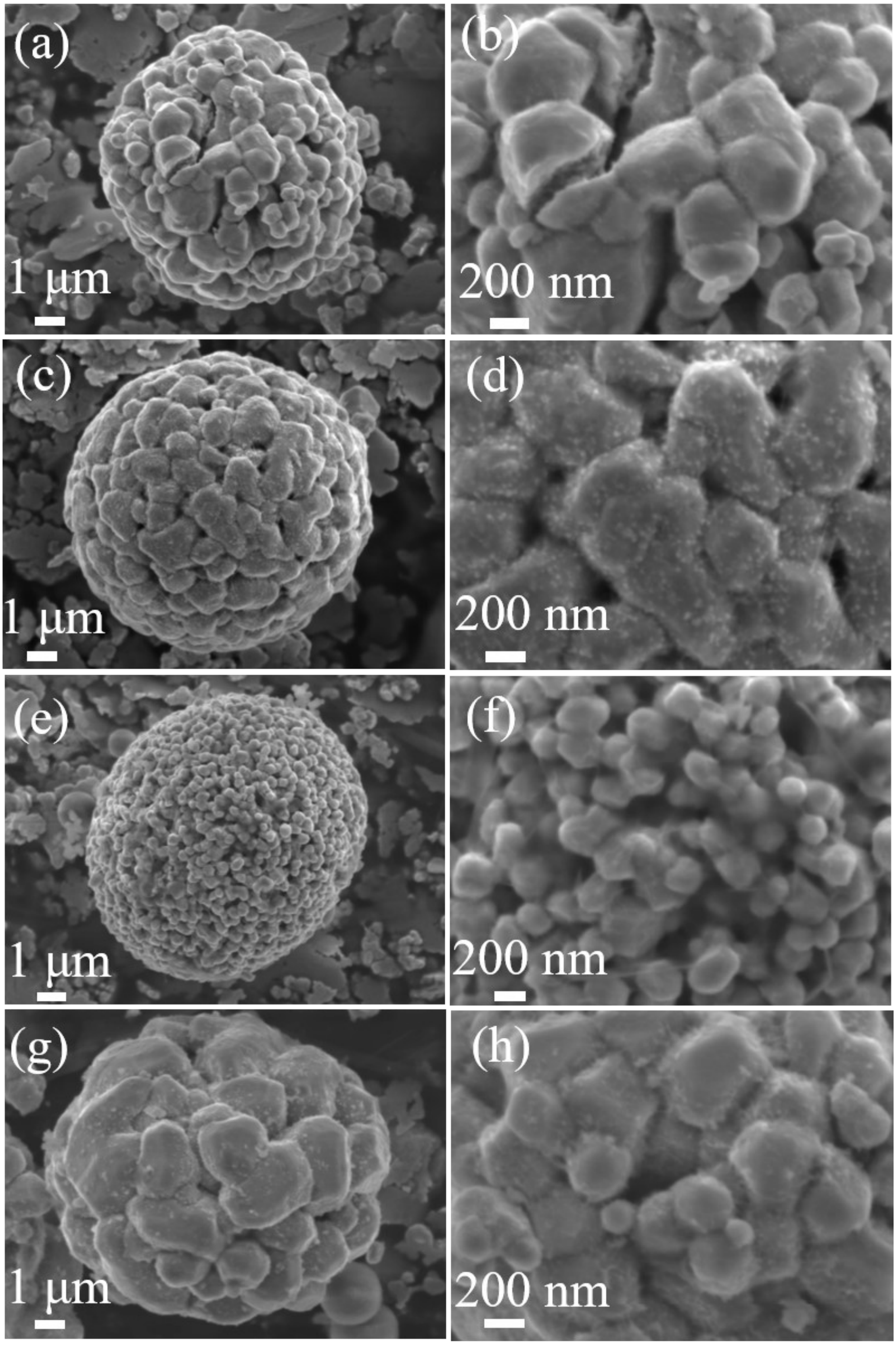

Figure S3 SEM images of (a, b) Co_3O_4-R-1, (c, d) Co_3O_4-R-3, (e, f) Co_3O_4-R-7, (g, h) Co_3O_4-R-9.

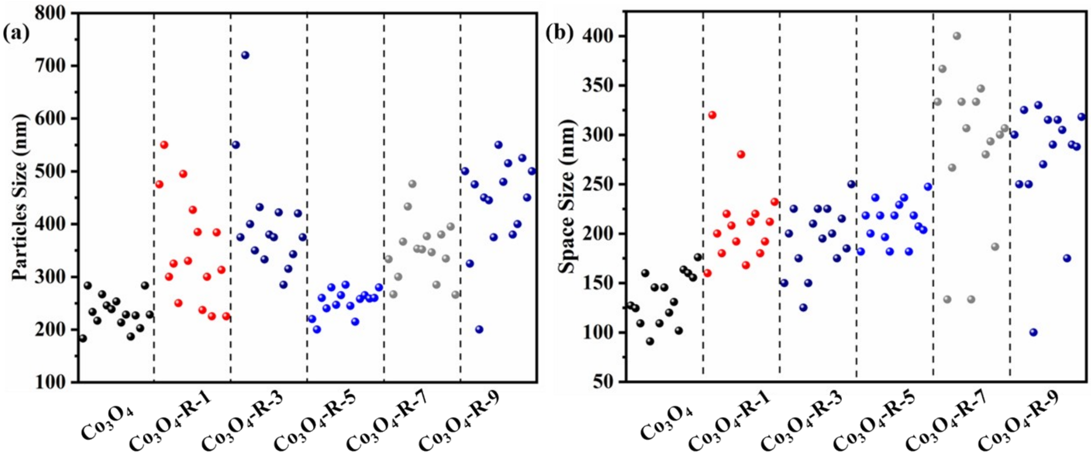

Figure S4 (a) The particle size and (b) space size of the nanoparticles in all the Co_3O_4 samples.

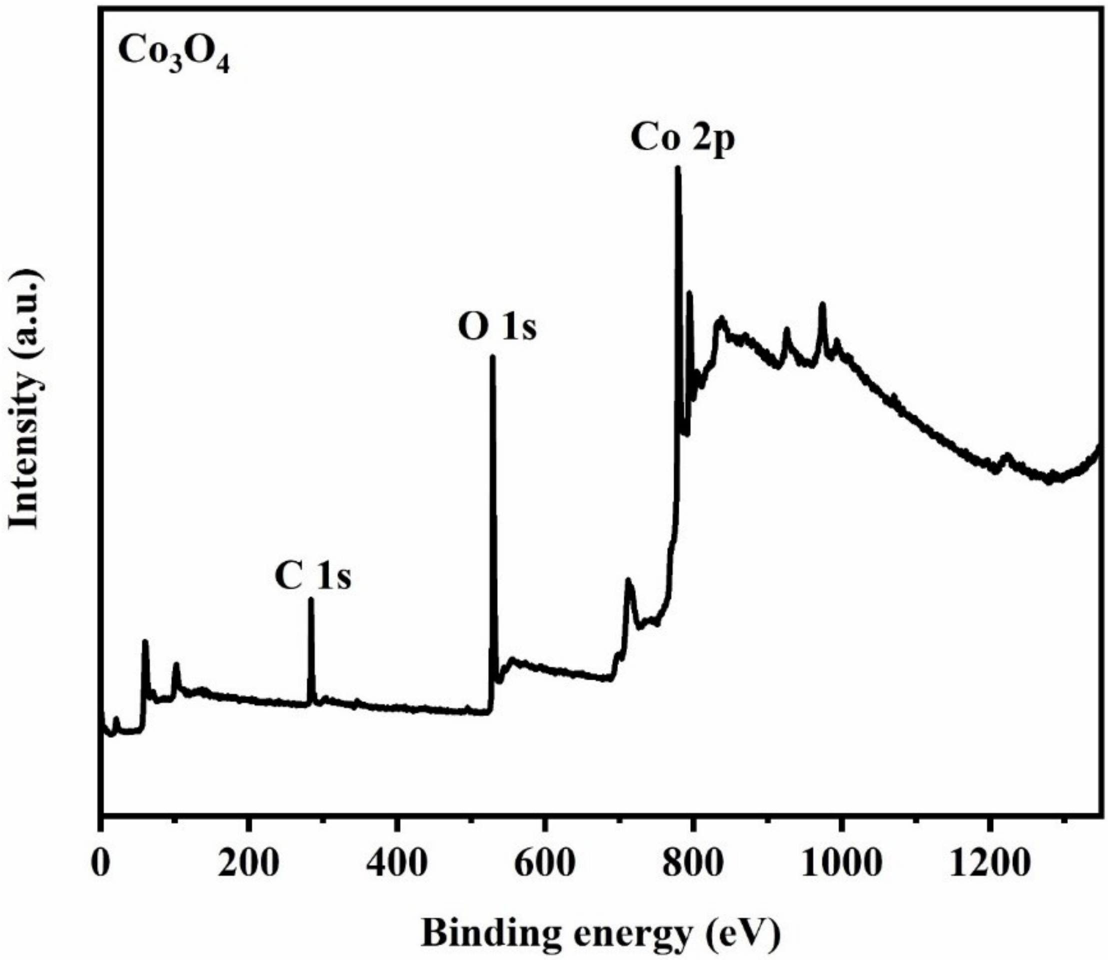

Figure S5 Wide-scan XPS spectrum of Co_3O_4.

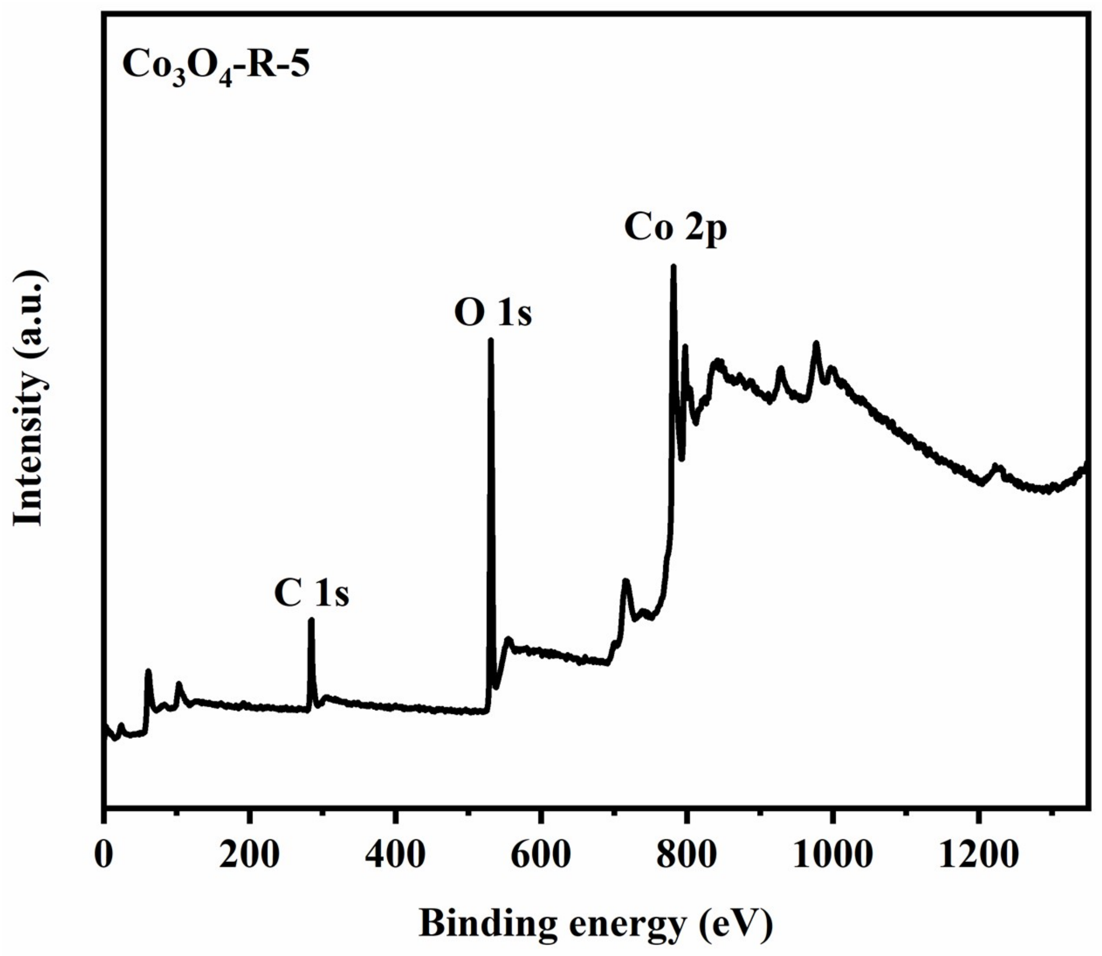

Figure S6 Wide-scan XPS spectrum of Co_3O_4-R-5.

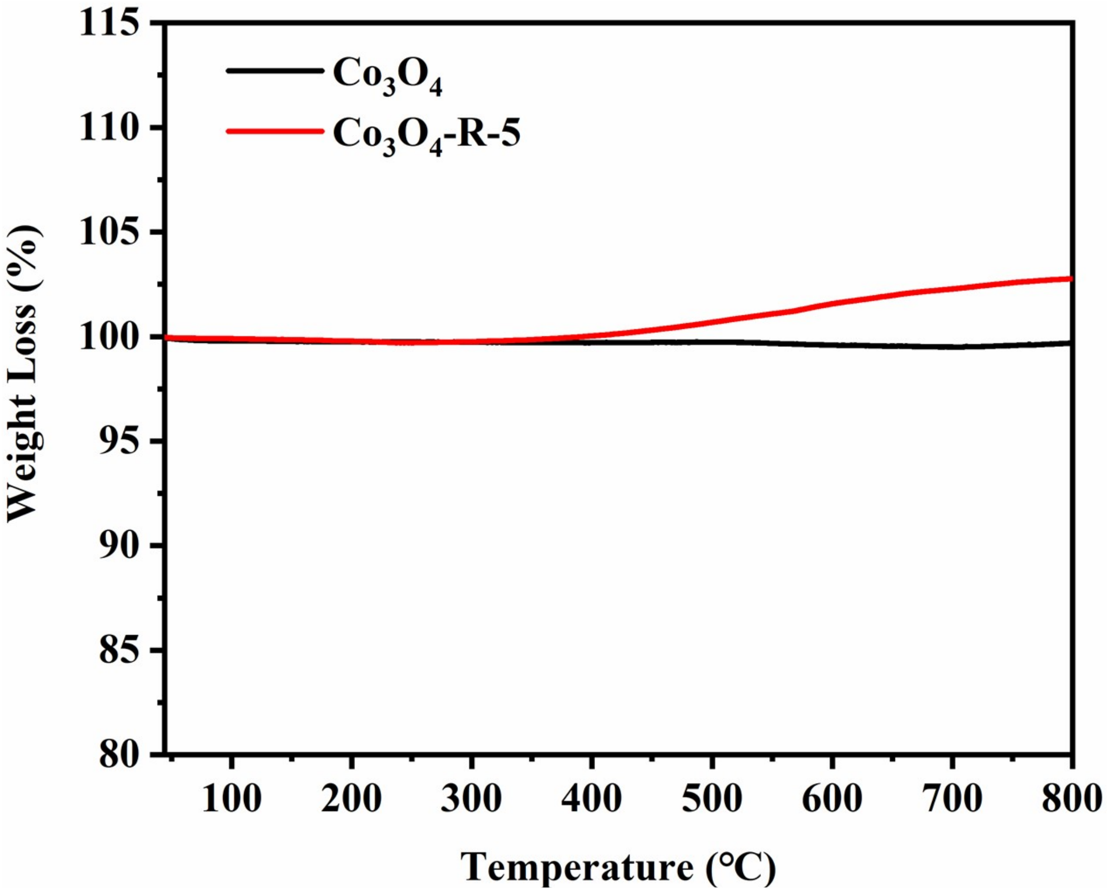

Figure S7 TGA curves of the Co_3O_4 and Co_3O_4-R-5.

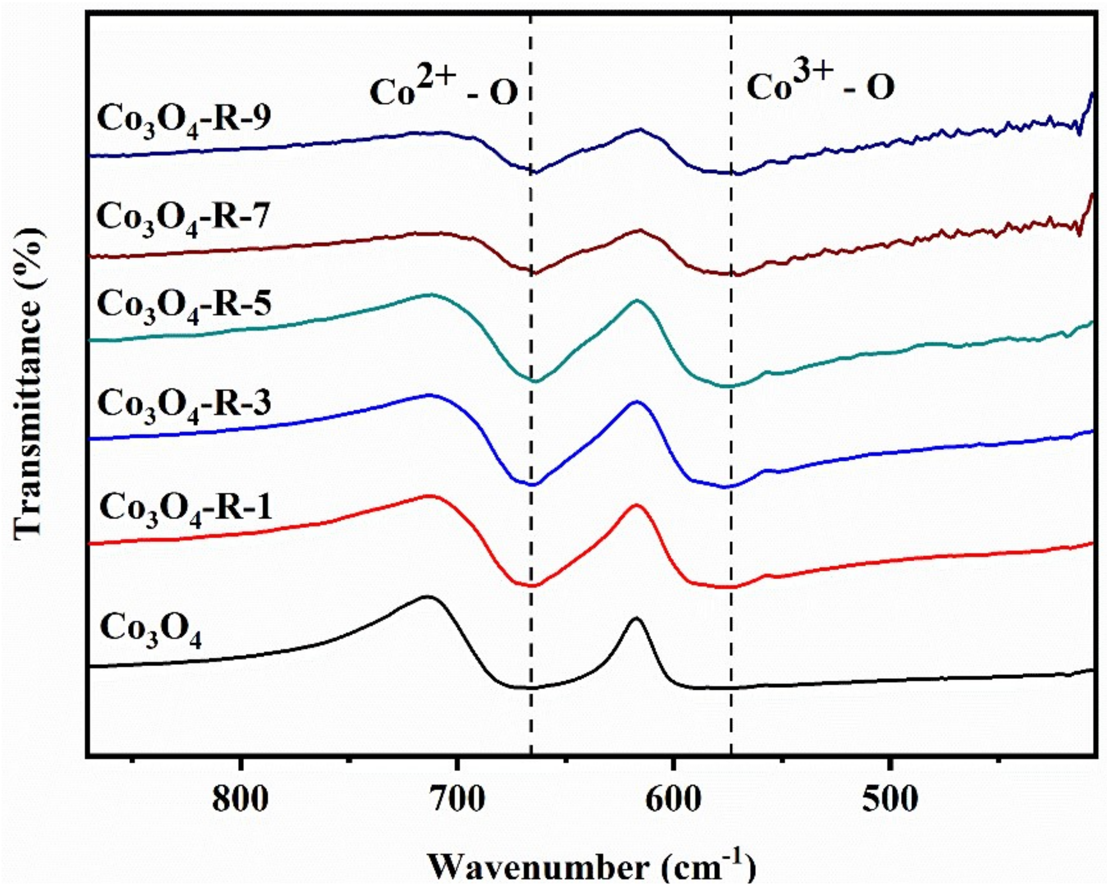

Figure S8 FT-IR spectra of Co_3O_4, Co_3O_4-R-1, Co_3O_4-R-3, Co_3O_4-R-5, Co_3O_4-R-7, Co_3O_4-R-9.

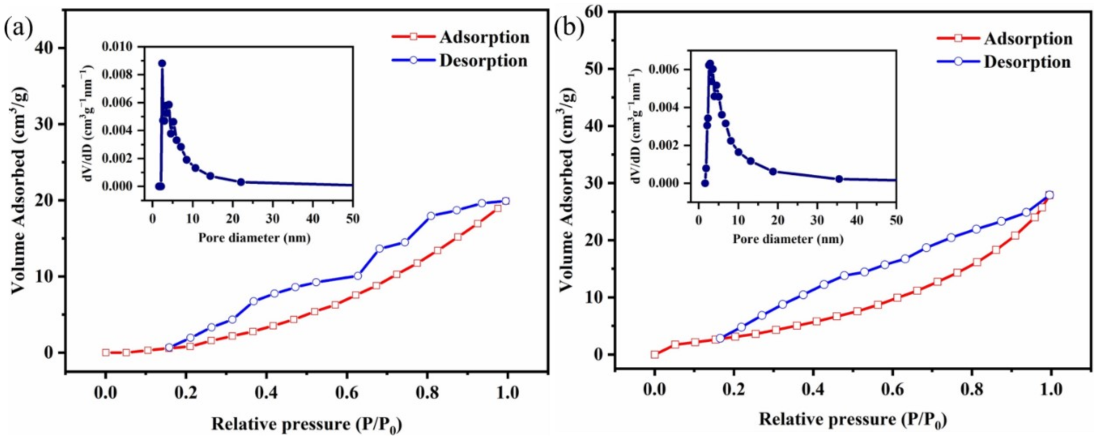

Figure S9 N_2 adsorption–desorption isotherms and pore size distribution curves of (a) Co_3O_4, (b) Co_3O_4-R-5 samples.

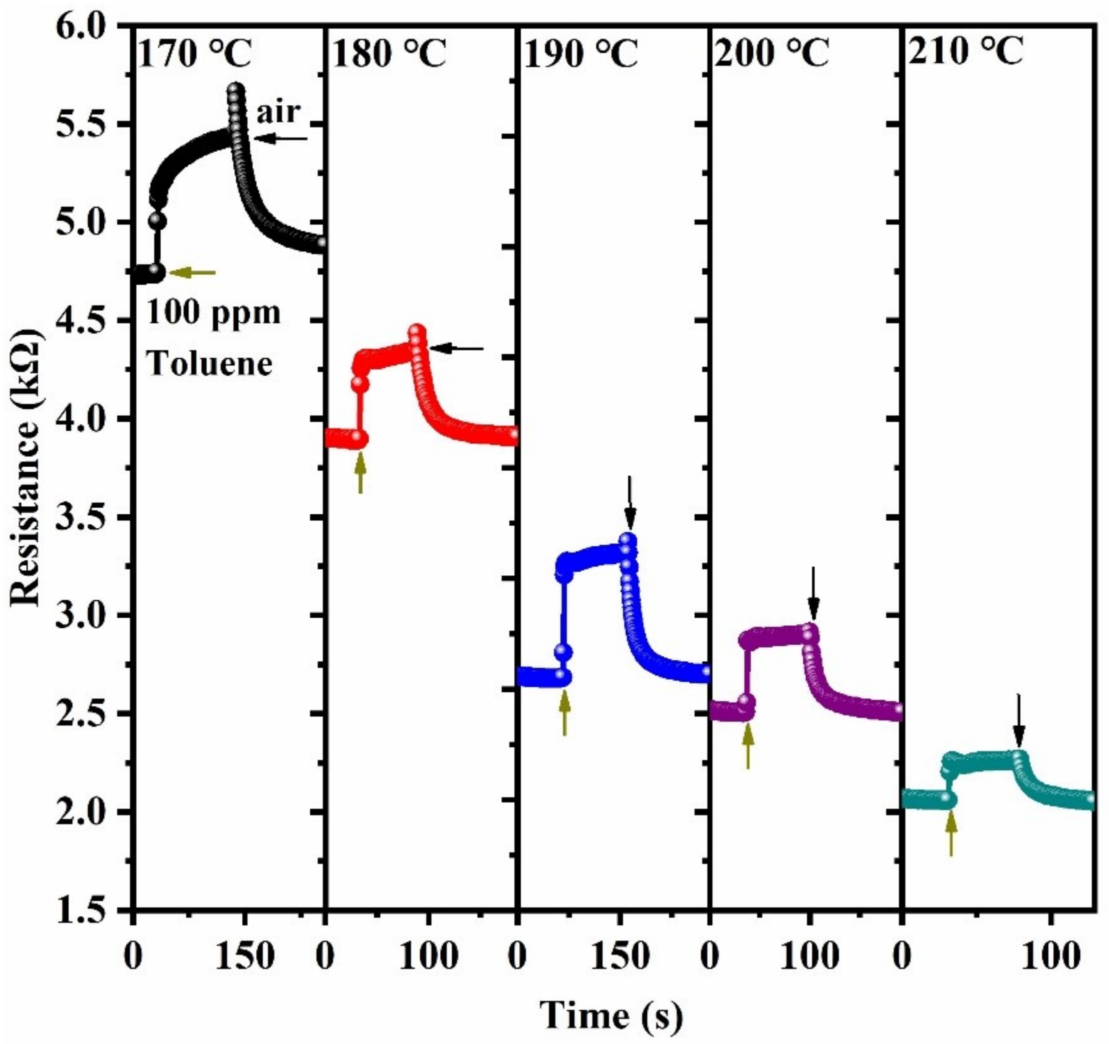

Figure S10 The response and recovery curves of Co_3O_4 sensors to 100 ppm toluene at 170 °C, 180 °C, 190 °C, 200 °C and 210 °C.

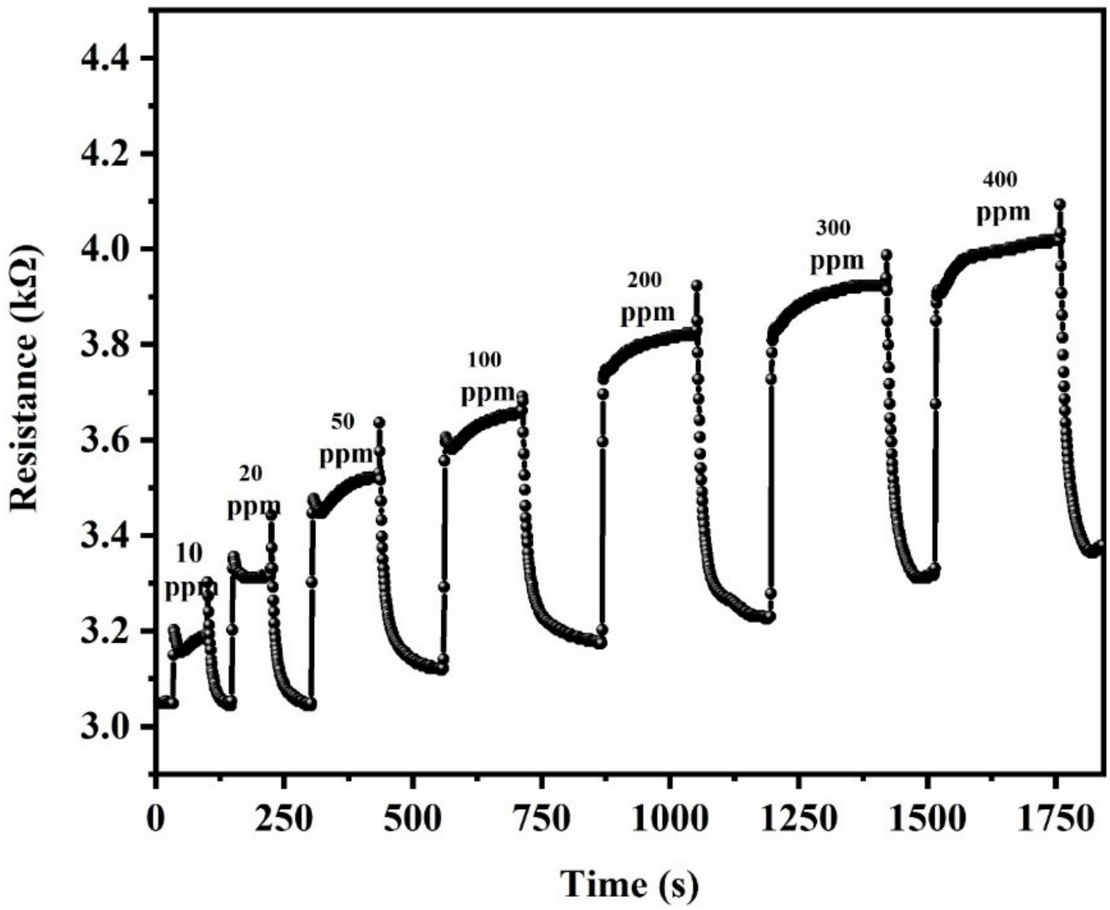

Figure S11 The response and recovery curve of Co_3O_4-based sensor to various toluene concentrations.